Magnetic and transport properties of a strongly anisotropic ferromagnet, UCu_2P_2

1990 J. Phys.: Condens. Matter 2 4185

(http://iopscience.iop.org/0953-8984/2/18/015)

J. Phys.: Condens. Matter **2** (1990) 4185–4196. Printed in the UK

Magnetic and transport properties of a strongly anisotropic ferromagnet, UCu_2P_2

D Kaczorowski and R Troć
W Trzebiatowski Institute for Low Temperature and Structure Research, Polish Academy of Sciences, 50-950 Wrocław, Poland

Received 16 October 1989

Abstract. We report here the results of the magnetisation and electrical resistivity measurements on UCu_2P_2 single crystals. This phosphide, crystallising in the hexagonal structure of $CaAl_2Si_2$ type, appears to be a strongly anisotropic ferromagnet with evidence of a significant domain effect at low temperatures. Its Curie temperature is as high as 216 K which is the record for any known ferromagnetic uranium compounds. The anisotropy field is of the order of magnitude of 10^6 Oe. The electrical resistivity results of UCu_2P_2 undoubtedly point to the semimetallic character of this compound. The character of magnetism in UCu_2P_2 as well as the origin of its very high T_c are discussed. We present also the magnetic ordering analysis based on the molecular-field approximation. As a result, we found four different magnetic structures which can occur for compounds with the $CaAl_2Si_2$-type crystal structure.

1. Introduction

In recent years the ternary rare-earth and actinide compounds with the general composition MT_2Z_2 (T ≡ transition metal; Z ≡ Si, Ge) have attracted much interest because of their intriguing physical properties. They usually crystallise with the derivatives of the tetragonal $BaAl_4$-type structure, such as the primitive $CaBe_2Ge_2$ or the body-centred $ThCr_2Si_2$ types (Parthé and Chabot 1984). A wide variety of unusual magnetic and electrical properties of these intermetallics is connected to the complex interactions of the localised magnetic moments of rare-earth or actinide atoms with the conduction electron band. As an example, it is enough to mention here the well known heavy-fermion compounds such as $CeCu_2Si_2$ (Steglich *et al* 1979) and URu_2Si_2 (Palstra *et al* 1985).

Although numerous groups of the corresponding rare-earth phases MT_2X_2 with pnictogen metalloids (X ≡ P, As, Sb, Bi) (Jeitschko *et al* (1988) and references therein) are known, the physical properties of these ternary compounds have not received much attention so far. Up to now, only the existence of a few uranium–transition-metal pnictides with 1:2:2 stoichiometry have been reported, e.g. UNi_2P_2 (Hofmann and Jeitschko 1984, Żołnierek *et al* 1986), $UNi_{2-x}As_2$ (Jeitschko *et al* 1988, Troć *et al* 1989), UCo_2P_2 and UFe_2P_2 (Jeitschko *et al* 1985, Kaczorowski 1989), UFe_2As_2 and UNi_2Sb_2 (Kaczorowski 1989), $URh_{2-x}As_2$ (Zemni *et al* 1988) and UCu_2P_2 (Żołnierek *et al* 1986). It is interesting to note that the first seven compounds crystallise with a tetragonal structure, while only the latter surprisingly adopts the hexagonal $CaAl_2Si_2$-type unit cell (Żołnierek *et al* 1987).

0953-8984/90/184185 + 12 $03.50

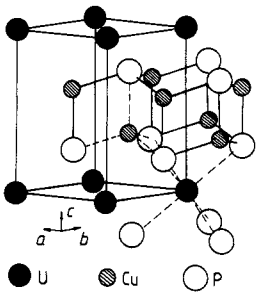

Figure 1. Crystal structure of UCu_2P_2: ---, coordination polyhedra of the uranium and copper atoms.

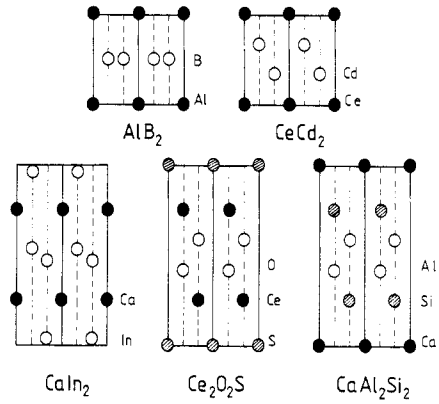

Figure 2. Comparison of the crystal structures of AlB_2, $CeCd_2$, $CaIn_2$, Ce_2O_2S and $CaAl_2Si_2$ types in the projection onto the a–c plane. The layered character of these structures is well apparent.

Some preliminary magnetic data on UCu_2P_2, based on measurements on polycrystalline samples, have already been reported previously (Żołnierek *et al* 1986). It appears that this phosphide is a ferromagnet with a Curie temperature as high as 216 K. Then, this temperature can be regarded as the highest for any uranium compound so far known, being a ferromagnet due to the coupling of uranium magnetic moments only. The powder magnetic susceptibility of this compound was fairly well approximated up to 900 K by a modified Curie–Weiss law with effective magnetic moment of $2.26\mu_B$ per U atom and $\theta_p = 212$ K. Recently, the temperature variations in the magnetic susceptibility components taken along and perpendicular to the c axis, $\chi_\parallel(T)$ and $\chi_\perp(T)$, respectively, have also been published (Kaczorowski 1988). In the present paper we report the results of the magnetisation and electrical resistivity measurements on UCu_2P_2 single crystals.

2. Crystallochemical considerations

UCu_2P_2 crystallises with the hexagonal $CaAl_2Si_2$-type structure (figure 1) that is an ordered version of the anti-La_2O_3-type structure. Its unit cell contains one formula unit, and the distribution of atoms is as follows: U, 1a (0, 0, 0); Cu, 2d ($\frac{1}{3}$, $\frac{2}{3}$, 0.63); P, 2d ($\frac{1}{3}$, $\frac{2}{3}$, 0.27).

The $CaAl_2Si_2$-type structure can be regarded as a distorted hexagonal close packing of the Si atoms, where the Ca atoms occupy half the octahedral holes and the Al atoms occupy a quarter of the tetrahedral voids (Hulliger 1979). The coordination polyhedra of the uranium (octahedra $[UP_6]$) and copper (tetrahedra $[CuP_4]$) atoms in UCu_2P_2, with D_{3d} and C_{3v} point symmetry, respectively, are slightly elongated along the c-axis. The $CaAl_2Si_2$-type unit cell reveals a typical layered character, and likewise other hexagonal lattices of AlB_2-, $CeCd_2$-, $CaIn_2$- and Ce_2O_2S-type structures and their derivatives (figure 2) with, common to all of them, a triangular net of atoms within the basal plane. For UCu_2P_2 the sequence of sheets normal to the c axis is U–P–Cu–Cu–P–U with the U–U separation in this direction being as large as 6.366 Å. Simultaneously,

this distance within the *a–b* plane is 3.941 Å. Hence, to the first approximation, UCu_2P_2 may be treated as a quasi-two-dimensional magnetic system. This structural feature gives rise to essential differences in the magnetic behaviour between UCu_2P_2 and the remaining uranium compounds crystallising with the hexagonal structures mentioned above.

In the course of intensive crystallochemical studies of the alkali-metal and rare-earth pnictides with the chemical formula MT_2X_2, Klüfers and Mewis (1977) have given a few requirements to be fulfilled in order to stabilise the $CaAl_2Si_2$-type structure. According to them, the fundamental features characterising such compounds are almost no bonding contacts between the metalloid atoms and a strong ionic character of the M–X bonds. They are normal valence compounds and can be rationalised as follows: $Ca^{2+}Al^{3+}Al^{3+}Si^{4-}Si^{4-}$ (Rühl and Jeitschko 1979). Therefore, for the copper-containing pnictides MCu_2P_2, this structure is possible only when M is a tetravalent ion (Klüfers *et al* 1979). Indeed, the compounds with $M \equiv Th^{4+}$ (Klüfers *et al* 1979), Zr^{4+} and Hf^{4+} (Lomnitskaya 1986) are all isostructural to $CaAl_2Si_2$, whereas those with $M \equiv Li^+$ (Mewis and Blumstengel 1978) and Ca^{2+} (Schleuger *et al* 1971) and La^{3+} (Klüfers *et al* 1979) adopt a tetragonal unit cell of the $ThCr_2Si_2$ type.

In the light of the above remarks, one can assign to UCu_2P_2 the following valence scheme: $U^{4+}Cu^{+}Cu^{+}P^{3-}P^{3-}$. Comparing the U–P and P–P distances in this compound (2.805 Å and 3.832 Å, respectively) with the respective sums of the atomic radii it becomes clear that the U–P bonding is really almost ionic and there is no bonding or at least very weak bonding between the phosphorous atoms themselves. On the other hand, the Cu–P bond lengths (about 2.4 Å) give rise to some interactions between these atoms (covalent bonding), resulting in a slightly lower real oxidation number of phosphorous than −3. These conclusions are also supported by the semimetallic character of UCu_2P_2, described later.

3. Experimental details

The polycrystalline samples of UCu_2P_2 were prepared by reacting the mixture of stoichiometric amounts of powdered copper metal and UP_2 in evacuated quartz ampoules for 2 weeks at 900 °C. The purity of the obtained specimens was checked by x-ray diffraction using a DRON 1.5 diffractometer and also by picnometric measurements in CCl_4. Single crystals of maximum dimensions 3 mm × 3 mm × 3 mm were obtained by the chemical vapour transport method using iodine as a transporting agent in a temperature gradient of 900–950 °C, as reported previously (Żołnierek *et al* 1987).

Magnetisation studies were performed on single-crystal specimens in the temperature interval 4.2–250 K and in applied magnetic fields up to 4 T using a moving-sample low-frequency magnetometer with a superconducting coil.

Electrical resistivity measurements were carried out in the temperature range 4.2–300 K using a conventional four-point DC technique. Ultrasonic welding was used for the first time in preparation of perfectly ohmic contacts to the specimens examined in these investigations.

4. Experimental results

4.1. Magnetic properties

Our magnetisation studies of UCu_2P_2 revealed that this compound orders ferromagnetically below 216 K. Figure 3 presents the magnetisation versus applied field

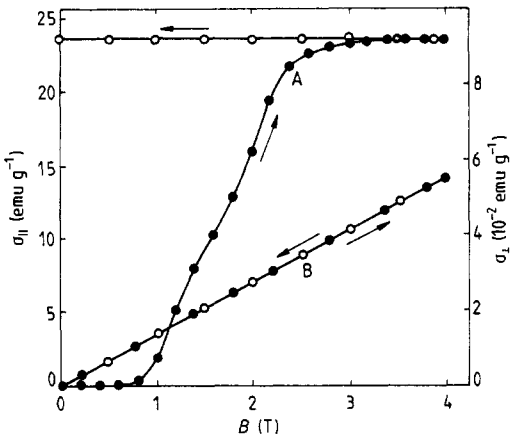

Figure 3. Magnetisation of UCu_2P_2 measured at 4.2 K and up to 4 T along ($\sigma_\parallel$) and perpendicular ($\sigma_\perp$) to the c axis: curve A, $\boldsymbol{H} \parallel \boldsymbol{c}$; curve B, $\boldsymbol{H} \perp \boldsymbol{c}$.

dependences measured at 4.2 K on a single crystal of UCu_2P_2 oriented either along ($\sigma_\parallel$) or perpendicular ($\sigma_\perp$) to the c axis of its hexagonal unit cell. As this figure indicates, UCu_2P_2 appears to be a very strongly anisotropic ferromagnet with the easy-magnetisation direction being along the crystallographic c axis. The magnetisation $\sigma_\perp$ taken within the basal plane is extremely low. Both a straight-line behaviour of $\sigma_\perp(H)$ and the absence of any hysteresis effect indicate that the transverse component of the spontaneous magnetic moment is equal to zero. Hence, it can be stated that the magnetic moments localised on the uranium atom sites are aligned along the c axis. The magnetisation $\sigma_\parallel(H)$ is already saturated at 4 T, reaching a value of 23.3 emu g^{-1} which corresponds to the magnetic ordered moment of 1.78 μ_B per U atom.

The uniaxial anisotropy energy E_a in the hexagonal lattice can be expressed as follows:

$$E_a = K_1 \sin^2\theta + K_2 \sin^4\theta + K_3 \sin^6\theta \cos(6\phi) \tag{1}$$

where K_1, K_2, K_3 are the anisotropy constants, while θ and ϕ denote the angles of the magnetisation vector with the c and b axis, respectively. In the case when the easy-magnetisation direction is parallel to the c axis, the magnetisation $\sigma_\perp$ within the basal plane measured in weak magnetic fields is given by

$$\sigma_\perp = (\sigma_s^2/2K_1)H \tag{2}$$

where σ_s is the spontaneous magnetisation.

From equation (2) we estimated for UCu_2P_2 the constant K_1 to be as large as 1.5×10^3 J kg^{-1} at 4.2 K; this corresponds to an anisotropy field H_A of about 10^6 Oe. Thus the magnetocrystalline anisotropy in UCu_2P_2 is of the same order of magnitude as that found before for the hexagonal intermetallic compound UGa_2 (Andreev *et al* 1979) as well as for the other phases with more ionic bonding UAsY (Y ≡ S, Se, Te) (Bazan and Zygmunt 1972, Bielov *et al* 1973) and U_3X_4 (X ≡ P, As) (see Zeleny (1981) and references therein; see also Troć *et al* (1981)).

A strong magnetocrystalline anisotropy usually results in the formation of very narrow Bloch walls. Hence, for UCu_2P_2 the occurrence of a large domain effect is also expected. Indeed, we found for this compound a high value of the nucleation field of the magnetisation—H_c = 0.7 T (see figure 3); this can be explained by the assumption of the formation of a compensated 180° type of domain structure which is rapidly reconstructed

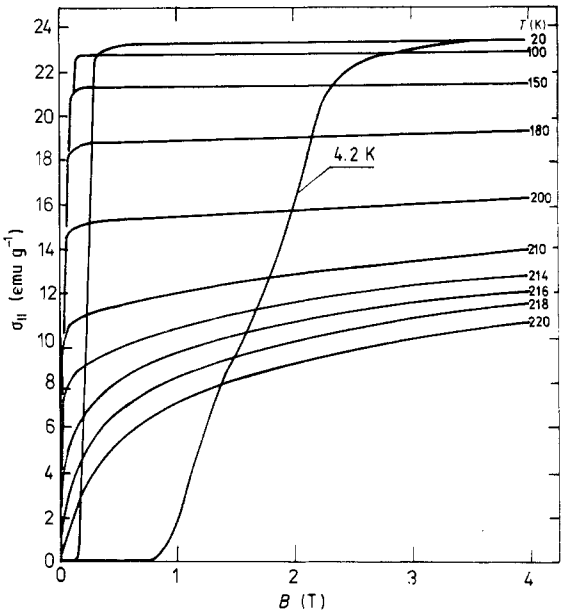

Figure 4. Magnetisation isotherms taken along the easy c axis ($\sigma_\parallel$) for UCu_2P_2.

at a field H_c. The untypical curvature of $\sigma_\parallel(H)$ observed in the vicinity of $H \simeq 2$ T might also be associated with a more complex domain effect. Clearly, UCu_2P_2 appears to be a magnetically very hard material with nearly 100% remanence and a wide hysteresis loop.

In figure 4 are shown selected magnetisation isotherms taken on a UCu_2P_2 single crystal at different temperatures below and above T_c. As can be seen, the $\sigma_\parallel(H)$ curves even at temperatures above T_c are not straight lines. This behaviour probably results from short-range magnetic interactions.

The $\sigma_\parallel(T)$ dependences, measured in the regimes of cooling sample with an applied field (field cooled (FC)) and without an applied field (zero field cooled (ZFC)) are presented in figure 5. Again, the shape of $\sigma_\parallel(T)$ is typical for a ferromagnet with a strong domain effect. A characteristic broad maximum occurring in $\sigma_\parallel(T)$ in the ZFC regime results from the competition between the domain movement induced by the temperature (leading to an increase in the magnetisation) and the thermal disorder in the magnetic moment system. Such a feature does not appear on the FC curve that may correspond to the measurement of $\sigma_\parallel(T)$ on a single-domain crystal.

The spontaneous magnetisation $\sigma_s(T)$ of UCu_2P_2 has been derived by the Arrott (1957) method. The obtained $\sigma_s(T)/\sigma_s(0) = f(T/T_C)$ variation is presented in figure 6, together with the theoretical functions derived in the molecular-field approximation (MFA) as well as in the 2D (Yang 1952) and 3D Ising (Guttman *et al* 1970) models. The calculations were performed for the effective spin $S = \frac{1}{2}$ appropriate for the assumption of the Γ_{3T} doublet as the crystal-field ground state in UCu_2P_2 (Kaczorowski 1988). As seen from figure 6, the experimental curve lies just between the theoretical results, but the 3D Ising model seems to describe the magnetic properties of UCu_2P_2 much better than the other models.

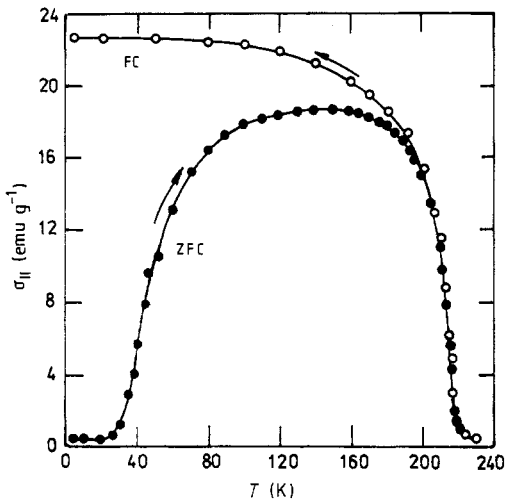

Figure 5. Temperature variation in the magnetisation of UCu_2P_2 measured in a field of 0.1 T applied along the c axis in the regimes of cooling the sample with an applied field (FC) and without an applied field (ZFC).

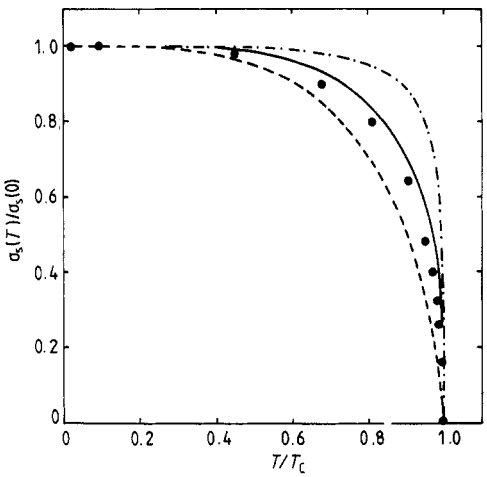

Figure 6. Reduced spontaneous magnetisation versus reduced temperature for UCu_2P_2: ●, experimental results; – – –, theoretical function corresponding to the MFA; —·—, theoretical function corresponding to the 2D Ising model; ——, theoretical function corresponding to the 3D Ising models.

4.2. Electrical resistivity

The results of the electrical resistivity measurements of single-crystal UCu_2P_2 are presented in figure 7. The shape of the $\rho_{\perp}(T)$ curve taken in the a–b basal plane is typical of many other semimetallic actinide or rare-earth ferromagnets but the value of the resistivity at room temperature is rather high, being equal to 1040 $\mu\Omega$ cm. In general, $\rho_{\perp}$ decreases with decreasing temperature down to the Curie temperature where it shows a 'kink' characteristic of the ferromagnetic materials. Then, $\rho_{\perp}$ decreases more rapidly, reaching a value of 91 $\mu\Omega$ cm at 4.2 K. The residual resistivity ratio (RRR) (defined as the ratio $\rho_{300K}/\rho_{4.2K}$) is 12. In turn, the resistivity $\rho_{\parallel}$ measured along the c axis displays a similar temperature variation, except for the region just below T_C. The curvature of the $\rho_{\parallel}(T)$ function in this temperature region is quite unusual, being rather a convex instead of the expected concave shape. For this case, the RRR is about 8 (ρ_{300K} = 920 $\mu\Omega$ cm and $\rho_{4.2K}$ = 113 $\mu\Omega$ cm). It is worthwhile noting that, in contrast to the huge magnetocrystalline anisotropy observed for UCu_2P_2 based on magnetic measurements, the anisotropy of the electrical resistivity is rather small. This feature is quite opposite to that found before, for example, in the case of UP_2 (Henkie and Trzebiatowski 1969).

In the inset in figure 7 we show the temperature derivatives of $\rho_{\perp}$ and $\rho_{\parallel}$ near the critical point. The ordering temperature defined as the extrema in the $\delta\rho_{\perp}/\delta T(T)$ and $\delta\rho_{\parallel}/\delta T(T)$ functions in both cases is 212 K. This value slightly differs from that determined in the magnetic measurements (216 K). This discrepancy is probably connected with the different sensitivities of magnetic and electrical measurements to short-range interactions.

All the experimental $\rho(T)$ curves were numerically analysed to identify various mechanisms of the conduction electron scattering processes, with an assumption that the Matthiessen rule is valid.

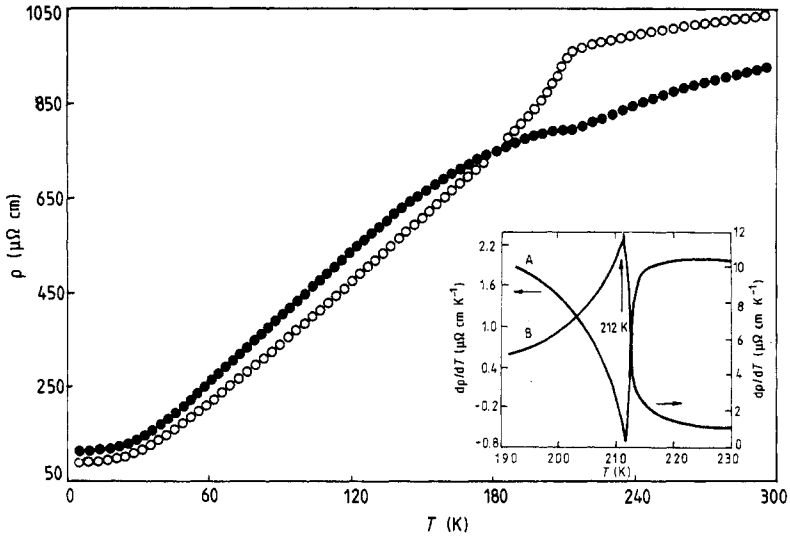

Figure 7. Electrical resistivities $\rho_{\parallel}$ (●) and $\rho_{\perp}$ (○) of UCu_2P_2 in the temperature range 4.2–300 K. The inset represents the corresponding temperature derivatives $d\rho_{\parallel}/dT$ (curve A) and $d\rho_{\perp}/dT$ (curve B) of the resistivity.

So, the temperature dependence of the resistivity below 70 K ($\simeq \frac{1}{3}T_C$) can be fairly well approximated by the equation

$$\rho(T) = \rho_0 + c_m T^2 \exp(-\Delta/T) \tag{3}$$

with the constants $\rho_0 = 91\ \mu\Omega$ cm, $c_m = 0.05\ \mu\Omega$ cm K^{-2} and $\Delta = 25$ K for transverse resistivity and $\rho_0 = 113\ \mu\Omega$ cm, $c_m = 0.06\ \mu\Omega$ cm K^{-2} and $\Delta = 26$ K for longitudinal resistivity. The first term in equation (3) denotes the residual resistivity, while the second term has a magnetic origin and describes the scattering processes of the electron–magnon type. The constant Δ here is the energy of the spin-wave excitation.

Fairly far above T_C, in the temperature range 260–300 K, both the components of the resistivity measured for UCu_2P_2 follow the formula

$$\rho(T) = \rho_0 + \rho_m^{\infty} + c_{ph} T \tag{4}$$

where $\rho_m^{\infty} = 758\ \mu\Omega$ cm, $c_{ph} = 0.64\ \mu\Omega$ cm K^{-1} and $\rho_m^{\infty} = 448\ \mu\Omega$ cm, $c_{ph} = 1.23\ \mu\Omega$ cm K^{-1} for $\rho_{\perp}$ and $\rho_{\parallel}$, respectively. In this function, apart from ρ_0 and the spin-disorder resistivity ρ_m^{∞}, an electron–phonon component appears also, which in accordance with the Grüneisen law is proportional to the temperature.

5. Magnetic ordering analysis

For determining the possible types of magnetic structure that can occur in the $CaAl_2Si_2$-type crystal structure, we have followed the method proposed by Smart (1966). This method, based on the MFA, was previously successfully used, for example, for discussing the magnetic ordering in uranium compounds crystallising with tetragonal crystal structures of either PbFCl (Przystawa and Suski 1967) or UGeTe type (Lorenc *et al* 1974).

Accordingly, in our calculations we consider the isotropic Heisenberg model of magnetic exchange. The whole crystal lattice of magnetic atoms we divide into n Néel sublattices in such a way that none of magnetic atoms is connected by exchange interactions to the other atoms within the same magnetic sublattice. Then, we introduce the molecular effective field $\boldsymbol{H}_i$ acting on the magnetic atom from the ith sublattice:

$$\boldsymbol{H}_i = \boldsymbol{H}_0 + \sum_{j=1}^{n} \gamma_{ij}\boldsymbol{M}_j \tag{5}$$

where $\boldsymbol{H}_0$ is the externally applied magnetic field, $\boldsymbol{M}_j$ denotes the magnetisation of the jth sublattice and γ_{ij} are the appropriate molecular-field constants defined by the formulae

$$\gamma_{ij} = n(2z_{ij}J_{ij})/Ng^2\mu_B^2$$

and (6)

$$\gamma_{ii} = 0$$

where J_{ij} denotes the integrals of exchange interactions of ith atom with jth neighbours, z_{ij} is the number of jth neighbours of the ith atom, and the remaining symbols have their usual meanings.

In the high-temperature approximation, $\boldsymbol{M}_i$ (which is in general a Brillouin function of $\boldsymbol{H}_i$) can be written as follows:

$$\boldsymbol{M}_i = (C/nT)\boldsymbol{H}_i, \tag{7}$$

where C is here the Curie constant of the localised 5f moments. The above formulae lead to a system of n linear equations for the sublattice magnetisations $\boldsymbol{M}_i$. In order to determine the temperature of magnetic phase transition we put $\boldsymbol{H}_0 = \boldsymbol{0}$. The obtained system of homogeneous linear equations has non-zero solutions for $\boldsymbol{M}_i$ only when its determinant is equal to zero. In this way it is possible to establish the expressions for the ordering temperatures corresponding to different types of magnetic ordering.

In the $CaAl_2Si_2$-type crystal structure, each magnetic atom has six nearest neighbours situated within the basal plane of the unit cell and two next-nearest neighbours located along the [001] direction on both sides of the plane. As already mentioned, the appropriate distances for UCu_2P_2 are equal to 3.941 Å and 6.366 Å, respectively. The successive nearest (third) uranium atom neighbours in UCu_2P_2 are placed at distances as large as 6.826 Å; so in the following the magnetic interactions more distant than between second neighbours will be neglected.

Thus, in our analysis we shall limit to two different exchange integrals J_1, J_2 and therefore we must divide the whole crystal lattice into six Néel sublattices, as shown in figure 8. Following the procedure described above, we have constructed the equation

$$\begin{vmatrix} 6T/C & -3\gamma_1 & -3\gamma_1 & -6\gamma_2 & 0 & 0 \\ -3\gamma_1 & 6T/C & -3\gamma_1 & 0 & -6\gamma_2 & 0 \\ -3\gamma_1 & -3\gamma_1 & 6T/C & 0 & 0 & -6\gamma_2 \\ -6\gamma_2 & 0 & 0 & 6T/C & -3\gamma_1 & -3\gamma_1 \\ 0 & -6\gamma_2 & 0 & -3\gamma_1 & 6T/C & -3\gamma_1 \\ 0 & 0 & -6\gamma_2 & -3\gamma_1 & -3\gamma_1 & 6T/C \end{vmatrix} = 0. \tag{8}$$

The solutions of this equation define possible expressions for the ordering temperatures T_C and T_N and they are as follows.

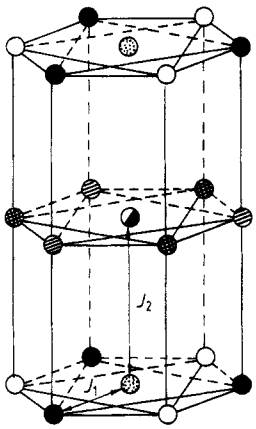

Figure 8. Crystal structure of UCu_2P_2 (two unit cells are shown) divided into six Néel sublattices. The magnetic atoms belonging to different sublattices are denoted by different symbols. The exchange interaction integrals J_1, J_2 are also shown.

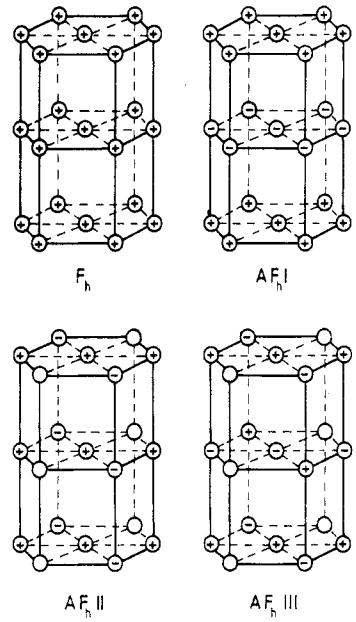

Figure 9. Possible magnetic structures for the compounds with the $CaAl_2Si_2$-type crystal structure: +, ferromagnetic coupling; −, antiferromagnetic coupling; ○, magnetic moments which cannot be correlated by the isotropic exchange interaction considered here (see text).

(i) For ferromagnetism F_h ($T_C = C(\gamma_1 + \gamma_2)$)

$$\boldsymbol{M}_1 = \boldsymbol{M}_2 = \boldsymbol{M}_3 = \boldsymbol{M}_4 = \boldsymbol{M}_5 = \boldsymbol{M}_6.$$

(ii) For antiferromagnetism, type AF_hI ($T_{N_1} = C(\gamma_1 - \gamma_2)$),

$$\boldsymbol{M}_1 = \boldsymbol{M}_2 = \boldsymbol{M}_3 = -\boldsymbol{M}_4 = -\boldsymbol{M}_5 = -\boldsymbol{M}_6.$$

(iii) For antiferromagnetism, type AF_hII ($T_{N_2} = C(-\frac{1}{2}\gamma_1 + \gamma_2)$),

$$\boldsymbol{M}_1 = -\boldsymbol{M}_2 = \boldsymbol{M}_4 = -\boldsymbol{M}_5 \qquad \text{and } \boldsymbol{M}_3 = \boldsymbol{M}_6$$

or

$$\boldsymbol{M}_1 = -\boldsymbol{M}_3 = \boldsymbol{M}_4 = -\boldsymbol{M}_6 \qquad \text{and } \boldsymbol{M}_2 = \boldsymbol{M}_5.$$

(iv) For antiferromagnetism, type AF_hIII ($T_{N_3} = C(-\frac{1}{2}\gamma_1 - \gamma_2)$),

$$\boldsymbol{M}_1 = -\boldsymbol{M}_2 = -\boldsymbol{M}_4 = \boldsymbol{M}_5 \qquad \text{and } \boldsymbol{M}_3 = -\boldsymbol{M}_6$$

or

$$\boldsymbol{M}_1 = -\boldsymbol{M}_3 = -\boldsymbol{M}_4 = \boldsymbol{M}_6 \qquad \text{and } \boldsymbol{M}_2 = -\boldsymbol{M}_5.$$

The corresponding magnetic structures are displayed in figure 9. One should note that the Néel temperatures T_{N_2} and T_{N_3} appear to be double roots of equation (8) and consequently the antiferromagnetic structures AF_hII and AF_hIII consist of two groups of uncorrelated sublattices (see figure 9).

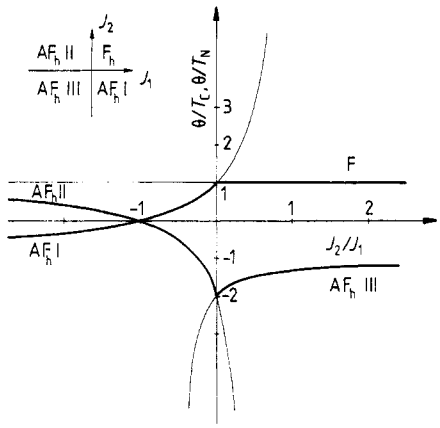

Figure 10. θ/T_C or θ/T_N ratio versus the relative strength J_2/J_1 of exchange interactions for the magnetic structures established in this work. The inset presents the stability diagram for these structures in the J_1–J_2 plane.

Assuming that the stable configuration has the highest ordering temperature, we were able to construct a stability diagram presented in the inset of figure 10. From this figure it follows that, when the exchange interactions J_1 within the basal plane are positive, the simple either ferromagnetic or antiferromagnetic structures arise depending on the sign of the exchange integral J_2 that couples the (001) layers of magnetic atoms. For a negative value of J_1, the magnetic moments within the (001) plane are 'frustrated'. In such a case, an anisotropic exchange interaction must be taken into account. Thus the simple molecular-field theory is insufficient for a full description of the magnetic structures being formed, i.e. AF_hII or AF_hIII.

It is worthwhile comparing the value of the paramagnetic Curie temperature defined as

$$\theta_p = \frac{C}{n}\sum_{j=1}^{n}\gamma_{ij} = \frac{2S(S+1)}{3k}\sum_{j=1}^{n} z_{ij}J_{ij} \tag{9}$$

with the values of the ordering temperatures T_C and T_N being established above. In figure 10 we put the θ_p/T_C or θ_p/T_N ratio as a function of the relative strength of exchange interactions J_2/J_1. One can see from this figure that, for the ferromagnetic configuration, θ_p is always equal to T_C but, in the case of antiferromagnets, θ_p can be either negative or positive and the θ_p/T_N ratio lies in the range from -2 to $+1$. It becomes clear that, for an antiferromagnetically ordered compound, θ_p is positive only when the exchange integrals between nearest neighbours (J_1) and next-nearest neighbours (J_2) in the crystal lattice have opposite signs (as is the case of the AF_hI- and AF_hII-type structures), and the ferromagnetic coupling is stronger than the antiferromagnetic coupling.

Furthermore, on the assumption that the exchange interactions between the second magnetic neighbours are negligibly weak ($J_2 \simeq 0$) it is possible to estimate an upper limit of J_1 from equation (9). In the case of UCu_2P_2 (for which such an assumption seems to be justified by a fairly large separation between the (001) planes), J_1 is as large as 72 K, reflecting the exceptionally high Curie temperature of this compound, originating mainly from the latter interaction.

6. The ordering temperature analysis

The most intriguing feature of UCu_2P_2 is the record value of its Curie temperature. It is worthwhile to remember here that the highest Néel temperatures among actinide

compounds known so far have been found for the U_2N_2X (X ≡ P, As) ternaries (T_N = 400 K and 363 K, respectively) which crystallise with a hexagonal structure of Ce_2O_2S type (Żołnierek and Troć 1976). The latter structure appears to be an antitype of that found for UCu_2P_2, i.e. $CaAl_2Si_2$. The main difference between these two structures is that in UCu_2P_2 the uranium atom layers are separated by four non-magnetic planes (P–Cu–Cu–P), whereas in the U_2N_2X-type compounds the uranium atom sheets are separated either by a single X plane or by double N–N planes (see figure 2). Moreover, in contrast to the two-dimensional character of the magnetic unit cell of UCu_2P_2, the two shortest U–U distances in the U_2N_2X compounds are almost the same. It is interesting to note that the U_2N_2X phases with X ≡ S, Se are also isostructural to Ce_2O_2S and exhibit antiferromagnetic ordering but their Néel temperatures are reduced by a factor of about 1.5 in comparison with the corresponding pnictides (Żołnierek and Troć 1976). Furthermore, such a compound but with X ≡ N, i.e. β-U_2N_3, is in turn ferromagnetic and its T_C (188 K) is only slightly lower than that of UCu_2P_2 (Trzebiatowski *et al* 1962).

Hence, one can conclude that in spite of almost the same U–U distances within the basal plane, characteristic of all the compounds discussed, the kind of ligand component plays probably the most important role both in the type of magnetic ordering being realised and in the magnitude of the critical temperature. In other words, the mechanism of superexchange in all these compounds seems to dominate any indirect exchange via conduction electrons (e.g. the RKKY-type interactions). Therefore any future theoretical analysis of the ordering temperatures of such actinide compounds must be based on the magnetic exchange mediated by ligands.

7. Concluding remarks

For crystallochemical reasons, UCu_2P_2 is thought of as a quasi-ionic compound with a rather well localised character of 5f electrons of the U^{4+} ions and therefore the magnetic data for this phosphide strongly reflect the local picture of its magnetism. For example, the very high Curie temperature together with the strong anisotropy found in both the ordered and the paramagnetic regions, the Curie–Weiss behaviour of the paramagnetic susceptibility as well as relatively high values of the ordered and effective magnetic moments all support the strongly localised character of the uranium 5f electrons in this compound. The high degree of the 5f-electron localisation in UCu_2P_2 has also been evidenced from the large positive effect of pressure on its T_C (Kaczorowski *et al* 1989) and from the magneto-optical spectroscopy data (Schoenes *et al* 1989).

Furthermore, the observed reduction in the values of the ordered and effective magnetic moments (1.78 μ_B per U atom and 2.26 μ_B per U atom respectively) result mainly from the crystal-field interactions on the U^{4+} ion (Kaczorowski 1988). In the latter paper the magnetic properties of UCu_2P_2 have been interpreted using a phenomenological approach based on the crystal-field model and the MFA. In this analysis a simplified doublet–singlet system of the lowest-lying crystal-field levels with an energy gap of about 500 K has been taken into account. It appears that such a system gives a quite good description of the magnetic behaviour of this compound in a wide temperature range.

In general, the magnetic ordering of the uranium moments in UCu_2P_2 arises as a result of the competition between the RKKY-type indirect exchange interaction and the superexchange via the metalloid anions. However, owing to the large distance between

the uranium atoms along the [001] direction, where they are separated by as many as four successive layers of non-magnetic atoms, we believe that the above exchange mechanisms operate mainly within the hexagonal (001) planes, in consequence leading to strong ferromagnetic coupling of the uranium magnetic moments within this plane. In addition, these mechanisms are influenced by a strong interaction of the uranium 5f electrons with the valence p electrons of the surrounding metalloids, probably in a similar way as in the case of cerium and uranium monopnictides (see, e.g., Takegahara *et al* 1981). Thus, this so-called p–f mixing interaction seems to be the origin of the huge magnetocrystalline anisotropy observed for UCu_2P_2.

Further studies with polarised neutrons, which can give more information above the complex magnetic nature of this compound, are now under way.

References

Andreev A V, Bielov K P, Deryagin A V, Levitin R Z and Menovsky A 1979 *J. Physique Coll.* **40** C4 82

Arrott A 1957 *Phys. Rev.* **108** 1394

Bazan C and Zygmunt A 1972 *Phys. Status Solidi* **12** 649

Bielov K P, Dmitrievskii A S, Zygmunt A, Levitin R Z and Trzebiatowski W 1973 *Zh. Eksp. Teor. Fiz.* **64** 582

Guttman A J, Domb C and Fox P E 1970 *J. Physique* **32** C1

Henkie Z and Trzebiatowski W 1969 *Phys. Status Solidi* **35** 827

Hofmann W K and Jeitschko W 1984 *J. Solid State Chem.* **51** 152

Hulliger F 1979 *Handbook on the Physics and Chemistry of Rare Earths* vol 4, ed K A Gschneider and L Eyring (Amsterdam: North-Holland) pp 153–235

Jeitschko W, Hofmann W K and Terbüchte L J 1988 *J. Less-Common Met.* **137** 133

Jeitschko W, Meisen U, Möller M and Reehuis M 1985 *Z. Anorg. (Allg.) Chem.* **527** 73

Kaczorowski D 1988 *J. Magn. Magn. Mater.* **76–7** 366

—— 1989 *Abs. 19èmes Journees des Actinides (Madonna di Campiglio, 1989)* p 55

Kaczorowski D, Duraj R and Troć R 1989 *Solid State Commun.* **70** 619

Klüfers P and Mewis A 1977 *Z. Naturf.* b **32** 753

Klüfers P, Mewis A and Schuster H U 1979 *Z. Kristallogr.* **149** 211

Lomnitskaya Ya F 1986 *Russ. J. Inorg. Chem.* **31** 40

Lorenc J, Przystawa J and Zygmunt A 1974 *Phys. Status Solidi* a **25** 637

Mewis A and Blumstengel P 1978 *Z. Naturf.* b **33** 671

Palstra T T, Menovsky A A, van den Berg J, Dirkmaat A J, Kes P H, Nieuwenhuys G J and Mydosh J A 1985 *Phys. Rev. Lett.* **55** 2727

Parthé E and Chabot B 1984 *Handbook on Physics and Chemistry of Rare Earths* vol 6, ed K A Gschneider and L Eyring (Amsterdam: North-Holland) pp 111–334

Przystawa J and Suski W 1967 *Phys. Status Solidi* **20** 451

Rühl R and Jeitschko W 1979 *Mater. Res. Bull.* **14** 513

Schleuger H, Jacobs H and Juza R 1971 *Z. Anorg. (Allg.) Chem.* **385** 177

Schoenes J, Fumagalli P, Rüegsegger H and Kaczorowski D 1989 *J. Magn. Magn. Mater.* **8** 112

Smart J S 1966 *Effective Field Theories of Magnetism* (Philadelphia, PA: Saunders)

Steglich F, Aarts J, Bredl C D, Lieke W, Meschede D, Franz W and Schäfer H 1979 *Phys. Rev. Lett.* **43** 1892

Takegahara K, Takahashi A, Yanase A and Kasuya T 1981 *Solid State Commun.* **39** 857

Troć R, Kaczorowski D, Noël H and Guerin R 1990 *J. Less-Common Met.* submitted

Troć R, Sznajd J, Novotny P and Mydlarz T 1981 *J. Magn. Magn. Mater.* **23** 129

Trzebiatowski W, Troć R and Leciejewicz J 1962 *Bull. Acad. Pol. Sci., Sér. Sci. Chim.* **9** 365

Yang C N 1952 *Phys. Rev.* **85** 808

Zeleny M 1981 *Czech. J. Phys.* B **31** 309

Zemni S, Vicat J, Lambert B, Madar R, Chaudouet P and Senateur J 1988 *J. Less-Common Met.* **143** 113

Żołnierek Z, Kaczorowski D, Troć R and Noël H 1986 *J. Less-Common Met.* **121** 193

Żołnierek Z, Noël H and Kaczorowski D 1987 *J. Less-Common Met.* **128** 265

Żołnierek Z and Troć R 1976 *Plutonium and Other Actinides* vol 1 ed H Blank and R Lindner (Amsterdam: North-Holland) p 589